Through-Thickness Tensile Properties of Triaxial Braided Composites

Jonathan A. Salem
Glenn Research Center, Cleveland, Ohio

Christopher Sorini
Arizona State University, Tempe, Arizona

NASA STI Program . . . in Profile

Since its founding, NASA has been dedicated to the advancement of aeronautics and space science. The NASA Scientific and Technical Information (STI) Program plays a key part in helping NASA maintain this important role.

The NASA STI Program operates under the auspices of the Agency Chief Information Officer. It collects, organizes, provides for archiving, and disseminates NASA's STI. The NASA STI Program provides access to the NASA Technical Report Server—Registered (NTRS Reg) and NASA Technical Report Server—Public (NTRS) thus providing one of the largest collections of aeronautical and space science STI in the world. Results are published in both non-NASA channels and by NASA in the NASA STI Report Series, which includes the following report types:

- TECHNICAL PUBLICATION. Reports of completed research or a major significant phase of research that present the results of NASA programs and include extensive data or theoretical analysis. Includes compilations of significant scientific and technical data and information deemed to be of continuing reference value. NASA counter-part of peer-reviewed formal professional papers, but has less stringent limitations on manuscript length and extent of graphic presentations.

- TECHNICAL MEMORANDUM. Scientific and technical findings that are preliminary or of specialized interest, e.g., "quick-release" reports, working papers, and bibliographies that contain minimal annotation. Does not contain extensive analysis.

- CONTRACTOR REPORT. Scientific and technical findings by NASA-sponsored contractors and grantees.

- CONFERENCE PUBLICATION. Collected papers from scientific and technical conferences, symposia, seminars, or other meetings sponsored or co-sponsored by NASA.

- SPECIAL PUBLICATION. Scientific, technical, or historical information from NASA programs, projects, and missions, often concerned with subjects having substantial public interest.

- TECHNICAL TRANSLATION. English-language translations of foreign scientific and technical material pertinent to NASA's mission.

For more information about the NASA STI program, see the following:

- Access the NASA STI program home page at http://www.sti.nasa.gov

- E-mail your question to help@sti.nasa.gov

- Fax your question to the NASA STI Information Desk at 757-864-6500

- Telephone the NASA STI Information Desk at 757-864-9658

- Write to:
  NASA STI Program
  Mail Stop 148
  NASA Langley Research Center
  Hampton, VA 23681-2199

NASA/TM—2019-220055

Through-Thickness Tensile Properties of Triaxial Braided Composites

Jonathan A. Salem
Glenn Research Center, Cleveland, Ohio

Christopher Sorini
Arizona State University, Tempe, Arizona

National Aeronautics and
Space Administration

Glenn Research Center
Cleveland, Ohio 44135

August 2019

Acknowledgments

Thanks to Chris Burke for machining test specimens and fixtures and running the tests.
Thanks to Subodh Mital for making the rules of mixtures estimates using pcGINA.

Through-Thickness Tensile Properties of
Triaxial Braided Composites

Jonathan A. Salem
National Aeronautics and Space Administration
Glenn Research Center
Cleveland, Ohio 44135

Christopher Sorini
Arizona State University
Tempe, Arizona 85281

Summary

The through-thickness strength of triaxial braided composites was measured using thin specimens bonded to metallic tabs. Despite providing reasonable engineering estimates of the bulk properties, some test specimen limitations were noted: Significant shear and tensile stresses occur and induce failure at the bond line for stronger epoxies; the strains over much of the exterior are ~10 percent lower than interior strains, which are representative of the nominal state; and non-bond-line failure often occurs near the first layer. These interferences were partially overcome by adding a large radius to the gage section. Based on finite element analysis and experimental measurements, the nominal through-thickness elastic modulus and Poisson's ratio are $E_{33} = 10.7$ GPa and $v_{31} = 0.08$, respectively, for the three triaxial braided, carbon fiber composites tested. Strengths vary from 14 to 40 MPa depending on the resin. Relative to the in-plane properties, the through-thickness modulus, fracture strength, failure strain, and Poisson's ratio are 1/5, 1/30, 1/6, and 1/4 of the values, respectively. Interlaminar failure occurred with varying degrees of fiber tear-out along with little damage to axial tows, resulting in a smooth undulating fracture surface. Attempts to avoid bond-line failure via stronger adhesives requiring postcure temperature excursions of 177 °C (350 °F) had little effect on elastic constants, but they reduced the strength of the E862-based composite severely. The strength of PR520- and 5208-based composites increased.

Introduction

A wide range of resins, fiber architectures, and manufacturing methods are available to make carbon fiber composite components. Triaxial braided composites employing large-tow-size yarns offer a good combination of cost and performance and thus are gaining usage in aerospace and automotive applications in which weight, protection, and cost are critical. One factor limiting the performance of such composites is due to the free tow ends: sections with terminated tow ends subjected to tensile loads exhibit low strength relative to sections with constrained tow ends. The failure mechanisms are tow splitting and delamination at edges subjected to load (Refs. 1 and 2). Centrally pressurized tubes, which have low stresses at free tow ends, exhibit comparable transverse and axial strengths (Ref. 2) by avoiding the failure mechanism.

A potential second limiter of performance and a less investigated property is the through-thickness strength, which is expected to be dominated by the relatively weak resin properties. The through-thickness strength is needed for simulation of complex structures, stress analysis of thick sections and prediction of impact damage to fan containment systems, because large through-thickness stresses can be developed. Further, an adequate materials database is needed (Ref. 3) for correlation to larger scale impact test results being used to develop and verify impact simulation models (Ref. 4), which is ongoing.

This study measures the out-of-plane strength and elastic constants for several common carbon/epoxy fiber composite systems manufactured as thin plates. Two specimen designs are compared and thereby provide out-of-plane properties for the systems.

Procedure

Composite panels were fabricated by North Coast Composites. Twelve layers of the 0°/+60°/–60° braid were used to make a composite panel. Each of the 12 layers were placed into a resin transfer mold (RTM) with the 0° fibers aligned in the same direction. Resin was then injected into the closed mold and cured according to processing conditions recommended by the resin manufacturer. Cured-panel dimensions (after trimming) were 0.6096 m (2 ft) wide by 0.6096 m (2 ft) long by 0.635 cm (0.25 in.) thick.

Material

High-strength, standard-modulus carbon fiber TORAYCA T700S (Toray Carbon Fibers America, Inc.) were used with three different 177 °C (350 °F) cure epoxy resins. Fiber properties as reported by the manufacturer are shown in Table I. The resins were selected to provide a range of toughness in the cured composites: (1) CYCOM PR520 (Cytec Industries, Inc.) is a one-part toughened resin specifically designed for the RTM process; (2) CYCOM 5208 (Cytec Industries, Inc.) is a one-part untoughened resin. This resin is not specifically marketed as an RTM resin, but its flow characteristics are suitable for RTM; and (3) EPIKOTE™ Resin 862/EPIKURE™ Curing Agent W system (Resolution Performance Products, now Hexion Specialty Chemicals) is a two-part, low-viscosity system that is easy to process because of its low viscosity and long working life at room temperature. This resin system will be designated E862 in this report. Table I lists the cured resin properties reported by each manufacturer. These properties are merely representative values since actual properties depend on the cure and postcure conditions used for various applications as well as the test specimen geometry, temperature, and strain rate. A more complete set of tension, compression, and shear data at various strain rates and temperatures for the E862 system is presented by Littell et al. (Ref. 1).

The two-dimensional triaxial braid preforms were fabricated by A&P Technology. The fiber architecture was a 0°/+60°/–60° triaxial braid. The 0° axial fibers were 24k flattened tows, and the ±60° bias fibers were 12k flattened tows.[1] Although larger fiber bundles were used in the axial direction, the fiber bundle spacings in the axial and bias directions were adjusted to give the same fiber volume in both the axial and bias directions. A unit cell of the braid architecture is shown in Figure 1, where the ±60° bias fibers are

TABLE I.—CARBON FIBER AND EPOXY
RESIN TENSILE PROPERTIES

Material	Elastic modulus, GPa	Failure strain, percent	Tensile strength, MPa
Fiber			
T700S	230	2.1	4,900
Resin			
PR520	4.00	----	82
5208	3.80	----	50
E862	2.70	~30[a]	61

[a]Failure strain exhibits strong dependence on strain rate and temperature.

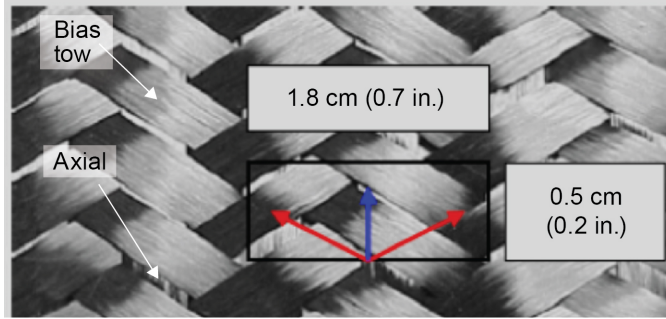[1]The terms "24k" and "12k" refer to the number of fibers in the fiber tow.

Figure 1.—Two-dimensional triaxial braid carbon fiber preform with highlighted unit cell. Blue arrow indicates axial tow direction, and red arrows indicate bias tow directions.

TABLE II.—TENSILE PROPERTIES OF CARBON/EPOXY FIBER COMPOSITES
[Values with ±1 standard deviation.]

Composite	Fiber fraction, percent	Axial direction				Transverse direction			
		Tensile strength, S_{f11}, MPa	Elastic modulus, E_{11}, GPa	Failure strain, percent	Poisson's ratio, ν_{12}	Tensile strength, S_{f22}, MPa	Elastic modulus, E_{22}, GPa	Failure strain, percent	Poisson's ratio, ν_{21}
T700S/PR520	55.9	1,035±34	47.6±1.1	2.16±0.09	0.31±0.02	599±3	42.8±1.6	1.68±0.19	0.30±0.003
T700S/5208	53.0	693±46	47.0±1.0	1.50±0.09	0.29±0.03	310±15	41.4±4.5	0.85±0.05	0.27±0.006
T700S/E862	55.6	800±63	46.9±1.6	1.78±0.08	0.30±0.03	462±36	41.4±4.5	1.44±0.09	0.29±0.020

visible on the surface, and portions of the 0° axial fibers that lie below the ±60° bias fibers are visible in the open spaces. Fiber volumes of the cured composites as measured using the acid digestion technique are summarized in Table II, along with the manufacturer's report properties. Table II also gives the in-plane properties of the composites, which are relatively isotropic, and indicates that the resin moduli and strength are more than an order of magnitude lower than the corresponding composite axial strength.

Specimen Geometry and Fixturing

The 25-mm- (1-in.-) diameter disks were diamond cored from 6.4-mm- (0.250-in.-) thick plates and lightly sanded with fine-grit-diamond paper to ensure good bonding with the adhesive and metallic load platens. The load stack was aligned via a v-block and cured per the manufacturer's recommendation.

The tests were performed following ASTM D7291 with the exception that the scope of D7291 does not cover coarse-braid composites, so the specimen diameter was kept greater than the largest dimension of the braid unit cell (18 mm, 0.7 in.). Although the usual test specimen is larger than the unit cell, size effects were checked by testing a set of 51-mm- (2.0-in.-) diameter specimens.

Test Method

Strains were initially monitored with three methods: strain gages, an extensometer, and photogrammetry. They were also predicted by using the rule-of-mixtures. In order to account for the extraneous signal from the extensometer, which was placed on the metal tabs, the properties of the loading tabs and the adhesive were considered to obtain the strain in the composite:

$$\varepsilon_C = \frac{\left(\Delta l_T - \varepsilon_{Fe} l_{Fe} - \varepsilon_A l_A\right)}{l_C} \tag{1}$$

where l_T is the total length of the section, ε is the strain, and *C*, *Fe*, and *A* designate the composite, steel, and adhesive sections, respectively.

Figure 2 and Table III compare the three methods. Because the adhesive behavior is very nonlinear and somewhat variable, estimates using Equation (1) were somewhat variable, and the method was abandoned in favor of strain gage measurements. Elastic modulus results using photogrammetry were similar to those from strain gages. However, the photogrammetry system was marginally adequate for determining Poisson's ratio because of the small strains and system resolution. Attention to detail in the setup resulted in a reasonable strain signal.

Results

Although the test results speak for themselves, finite element analyses discussed in this section illustrate improvements that can be made to the design of thin test specimens, and how changes in surface strain with specimen geometry affect elastic modulus estimates.
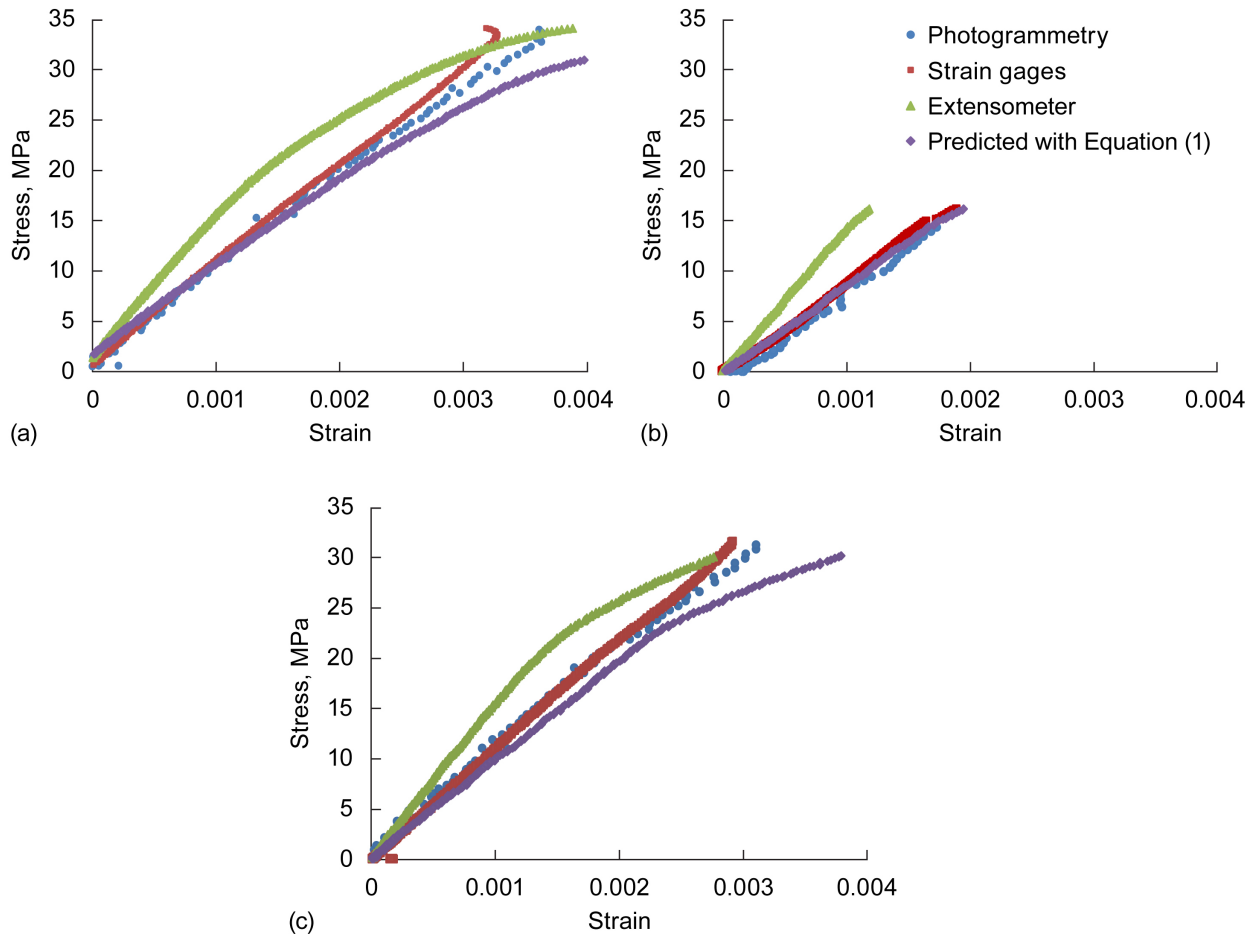

Figure 2.—Stress-strain diagrams for various strain measurement methods for T700S carbon fiber triaxial braided composites with different epoxy resins. (a) PR520. (b) 5208. (c) E862.

TABLE III.—THROUGH-THICKNESS PROPERTIES OF CARBON/EPOXY FIBER
COMPOSITES VIA DIFFERENT STRAIN MEASUREMENT METHODS
[Values with ±1 standard deviation.]

Composite	Elastic modulus, E_{33}, GPa				Poisson's ratio, $\nu_{31} \approx \nu_{32}$	
	Predicted[a]	Extensometer[b]	Photogrammetry	Strain gage	Strain gage	Photogrammetry
T700S/PR520	8.6	9.5±1.0	10.6±1.0	10.5±0.05	0.08±0.02	0.08±0.01
T700S/E862	8.1	8.2± 2.0	10.5±1.3	10.3±0.7	0.08±0.02	-----------

[a]Using the rule-of-mixtures.
[b]Using Equation (1).

TABLE IV.—THROUGH-THICKNESS TENSILE PROPERTIES
OF CARBON/EPOXY FIBER COMPOSITES
[Values with ±1 standard deviation.]

Composite	Out-of-plane direction			
	Tensile strength, S_{f33}, MPa	Elastic modulus, E_{33}, GPa	Failure strain, percent	Poisson's ratio, $\nu_{31} \approx \nu_{32}$
T700S/PR520	40.7±2.4	10.5±0.7	0.41±0.08	0.08±0.02
T700S/5208	14.0±1.7	11.0±0.8	0.15±0.05	0.07±0.01
T700S/E862	36.5±2.1	10.3±0.7	0.36±0.06	0.08±0.02

Strength

The test results are summarized in Table IV. Respectively, the elastic modulus, fracture strength, failure strain, and Poisson's ratio are 1/5, 1/30, 1/6, and 1/4 of the in-plane axial values. For all three materials, the elastic modulus, E_{33}, was approximately 10.7 GPa as measured, and Poisson's ratio relating the out-of-plane strain to in-plane strain was small, on the order of $\nu_{31} = 0.08$, implying that $\nu_{13} \approx \nu_{23} \approx 0.4$ (per Betti's reciprocal theorem).

Noteworthy was the location of failure for the T700S/PR520 and T700S/E862 specimens: failure almost invariably occurred at the bond line or about the first and second layers, as though the top layer(s) was torn off (Figure 3(a)). Although stronger bonding adhesives could be used to avoid bond-line failures, the required cure temperatures usually exceeded the transition temperature of the epoxy. Testing using one such cure indicated substantial changes in strength, as shown in Table V.

The stress-strain diagrams occasionally exhibited load-relaxation just before failure (Figure 3(a)), also implying that failure initiated at the perimeter of the exterior-most (top or bottom) layers, between which the strain gages sat. Per the ASTM D7291 failure location requirements, tests for 90 percent of the T700S/PR520 specimens were invalid as were tests for 50 percent of the T700S/E862 specimens.

In contrast, the failure behavior of the relatively weak T700S/5208 specimens was linear and often located near the central plane of the specimen thickness, as shown in Figure 3(b). It is speculated that the adhesive, which is relatively flexible ($E = 1.11$ GPa, $\nu = 0.34$), was contracting and squeezing the top layers sufficiently to add shear to the desired tensile stress, essentially popping off the top layer. For T700S/5208 it is speculated that either the tensile strength was exceeded prior to the shear strength or the central region was particularly weak.
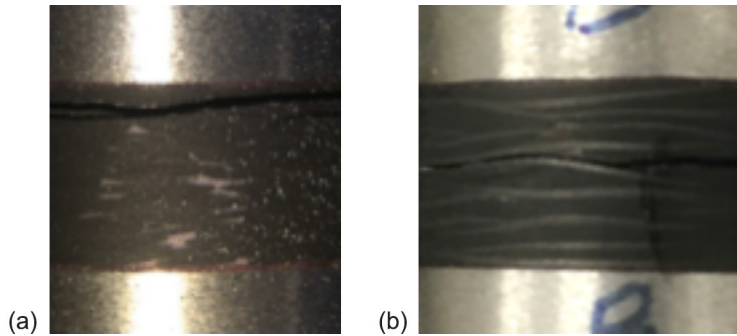
(a)   (b)

Figure 3.—Common failure locations in straight-sided T700S carbon
fiber composites with different epoxy resins. (a) PR520. (b) 5208.

TABLE V.—EFFECT OF EXCESSIVE CURE TEMPERATURE ON THROUGH-THICKNESS
TENSILE PROPERTIES OF T700S/PR520 CARBON/EPOXY FIBER COMPOSITE
[Values with ±1 standard deviation.]

Gage section geometry	Cure temperature, °C	Out-of-plane direction				Failure type[a]
		Tensile strength, S_{f33}, MPa	Elastic modulus, E_{33}, GPa	Failure strain, percent	Poisson's ratio, $\nu_{31} \approx \nu_{32}$	
Radiused	177	52.8±0.5	10.6±0.5	0.56±0.02	0.04±0.03	MG (valid)
Straight	177	39.9±2.7	----------	------------	------------	Bond line
Radiused	107	40.7±2.4	10.5±0.7	0.41±0.08	0.08±0.02	MG (valid)

[a]MG indicates multiple failure planes within the gage section.

In order to avoid failure near the tabs, the standard geometry was modified to include a large radius that reduced the central section diameter to 25.1 from 25.4 mm (0.99 from 1.00 in.). These specimens will be referred to as "radiused" specimens. This successfully moved failure away from the bond line, thereby producing valid tests per ASTM D7291, although making little difference in measured strength, as shown in Table VI. However, the elastic modulus tends to be slightly lower, as shown in Table VII. Table VIII summarizes Poisson's ratio results for the composites. Noteworthy is the difference in stress-strain curves for the stronger materials: Nonlinear behavior is exhibited at much lower loads, as seen in Figure 4. In the straight-sided specimens, failure often initiated above the strain gages, making the readings less sensitive to material failure behavior. Use of a higher-temperature cure adhesive (177 vs. 107 °C), which affected the material strength, yielded typical strengths and bond-line failure for straight-sided specimens, whereas radiused specimens allowed strengths as large as 50 MPa to be measured without bond-line failures. The overall mean strengths given in Table IV and Table VI are best estimates made by combining the valid tests and invalid tests that exceed the strength of valid tests. This should provide a better estimate by minimizing bias due to the strongest result being truncated by bond-line failure.

Larger, 51-mm- (2-in.-) diameter T700S/5208 straight-sided specimens exhibited similar strength to that of smaller 1-in.-diameter specimens, implying little effect of test specimen volume.

Finite Element Analysis

In order to understand the observed failure mode, finite element analysis (FEA) was performed with the commercial finite element code ABAQUS/Standard (Dassault Systèmes) using an orthotropic, smeared homogeneous model with the composite represented with 12 layers of solid elements (1 for each layer in the composite). An adhesive layer was represented with three layers of solid elements and the corresponding isotopic elastic properties. Mesh density was varied to ensure reasonable convergence.

TABLE VI.—THROUGH-THICKNESS TENSILE STRENGTH
FOR VARIOUS TEST CONFIGURATIONS OF
CARBON/EPOXY FIBER COMPOSITES
[Values with ±1 standard deviation.]
[Ratio of valid to total specimens tested in given parenthesis.]

Gage section geometry	Tensile strength, $S_{f\,33}$, MPa		
	T700S/PR520	T700S/5208	T700S/E862
Straight			
Batch 1	35.1±14 (0/3)	12.9±1.1 (3/3)	33.8±9.1 (1/3)
Batch 2	34.8±3.5 (1/8)	14.8±1.4 (8/8)	32.0±4.1 (4/7)
51-mm diam.	----------------	12.3±1.5 (4/4)	-----------------
Radiused	40.8±1.0 (4/4)	13.0±2.1 (3/3)	35.2±1.6 (3/3)
Overall mean	40.7±2.4	14.0±1.7	36.5±2.1

TABLE VII.—THROUGH-THICKNESS ELASTIC MODULUS
FOR VARIOUS TEST CONFIGURATIONS OF
CARBON/EPOXY FIBER COMPOSITES
[Values with ±1 standard deviation.]

Gage section geometry	Elastic modulus, E_{33}, GPa		
	T700S/PR520	T700S/5208	T700S/E862
Straight			
Batch 1	11.1	11.7	11.0
Batch 2	10.1±0.4	10.9±0.4	9.7±0.1
51-mm diam.	10.4±0.8	11.0±1.0	10.3±0.9
Radiused	----------	10.9±0.8	----------
Overall mean	10.5±0.5	11.0±0.8	10.3±0.7

TABLE VIII.—THROUGH-THICKNESS POISSON'S RATIO
FOR VARIOUS TEST CONFIGURATIONS OF
CARBON/EPOXY FIBER COMPOSITES
[Values with ±1 standard deviation.]

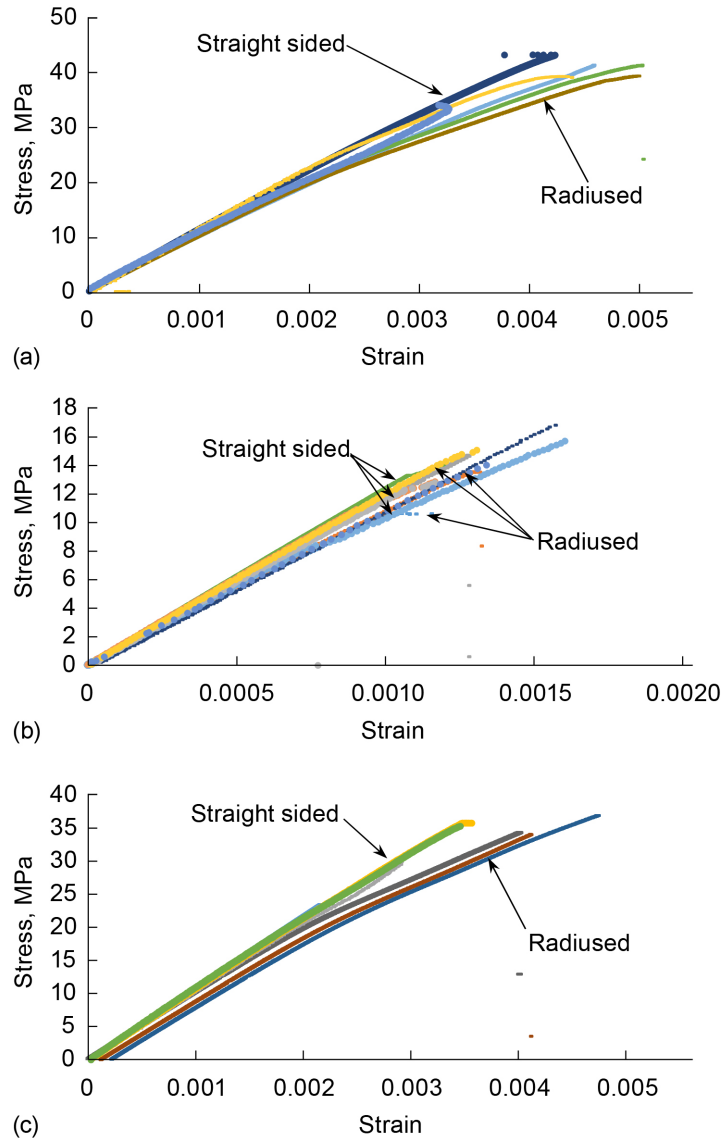| Gage section geometry	Poisson's ratio, $\nu_{31} \approx \nu_{32}$		
	T700S/PR520	T700S/5208	T700S/E862
Straight			
Batch 1	------------	------------	------------
Batch 2	0.06±0.02	0.08±0.05	0.09±0.02
51-mm diam.	0.09±0.03	0.06±0.01	0.06±0.04
Radiused	------------	0.07±0.05	------------
Overall mean	0.08±0.02	0.07±0.01	0.08±0.02

Figure 4.—Effect of specimen geometry on stress as function of strain for T700S carbon fiber composites with different epoxy resins. (a) PR520. (b) 5208. (c) E862.

The results shown in Figure 5 for a straight-sided specimen at a nominal tensile stress of 35 MPa (corresponding to the PR520 tensile strength) confirm the presence of a ±4-MPa in-plane shear between the first layer and bond layer where the bias and axial tows intersect the specimen machined perimeter. The peak tensile stress in and around the first layer is also higher by ~4 percent, implying that failure is likely to initiate at the region of increased combined shear and tension, especially if the shear strength is low. Further, over much of the exterior surface, the tensile strains are about 6 percent lower than within the bulk, implying that surface strain measurements overestimate the elastic modulus. A 6:1 ratio of tensile stress to shear stress occurs at maxima locations. As shown in Figure 6, photogrammetry images of the straight-sided test specimens confirm the surface strain distribution of the FEA. If the surface derived strain measurement are increased by 6 percent, as implied by FEA, then better agreement occurs between various strain methods and the rule-of-mixtures, as can be seen in Table III. Another important factor not accounted for in this FEA is thermal stresses induced during cooling from curing.
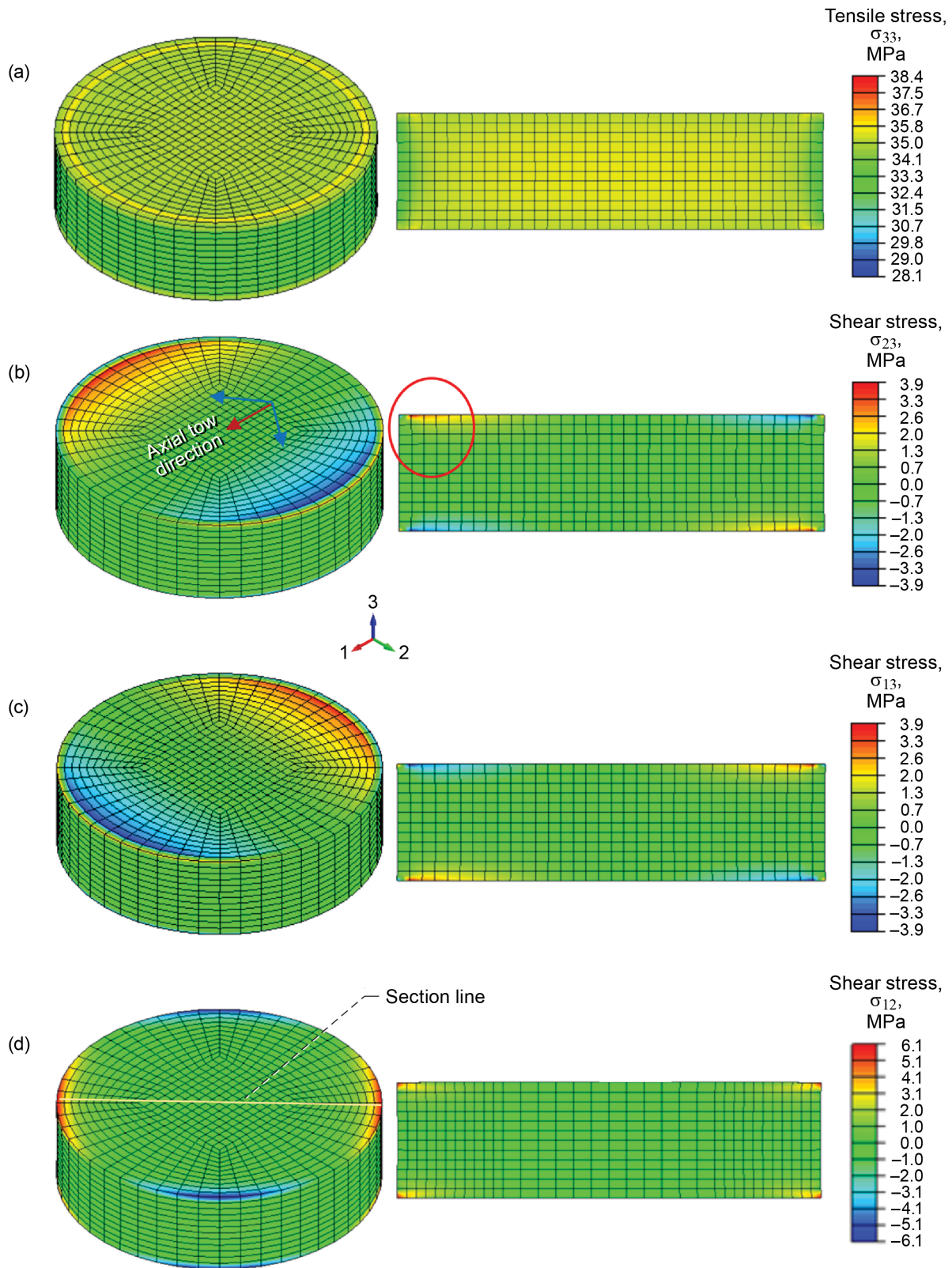
Figure 5.—Finite element analysis of straight-sided carbon/epoxy fiber composite. Tensile and shear stress distributions for global axial σ_{33} (Z) stress of 35 MPa. (a) σ_{33} stresses on perimeter and through the section. (b) σ_{23} shear stresses in first and second layers. (c) σ_{13} stresses. (d) σ_{12} stresses.
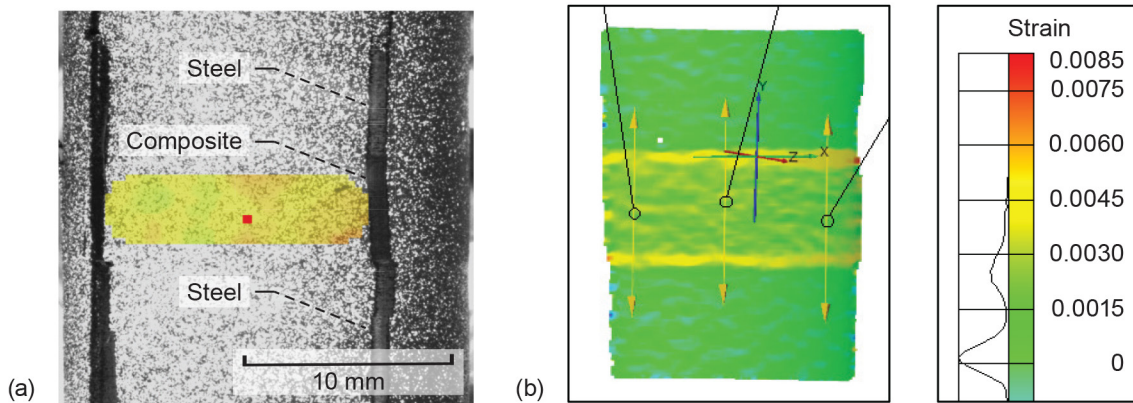
Figure 6.—Surface strain distribution of T700S/E862 fiber composite. (a) Photogrammetry image. (b) Finite element analysis showing increased strain near specimen edges and bond line.

A simple criteria for determining applicability of such a state to estimate the through-thickness strength is that the tensile stress σ_f must significantly exceed the tensile strength S_f prior to the shear strength of the epoxy or adhesive T_f being exceeded by shear stress τ_f:

$$\frac{\sigma_f}{S_f} > \frac{\tau_f}{T_f} \tag{2}$$

If the shear strength and tensile strength of the epoxies are similar (as determined in Ref. 5), the criteria are likely to be met, and shear-induced failure is unlikely. The shear strength of the adhesive is currently unknown.

FEA results for the radiused specimen are shown in Figure 7, and Figure 8 compares stresses between the designs. As with straight-sided specimens, tensile stress concentrations exist at the center of the gage section, with the difference being a surface concentration for the radiused design. The shear stresses remain similar. The normal stress at the interface is slightly lower than in the nominal state, allowing failure stress on the order of 50 MPa without bond-line failure (Table V). Although it is simplest to use a straight-sided specimen and reduce the modulus by ~6 percent, bond-line failure needs to be avoided if strength is to be measured. If bond-line failure cannot be avoided, then the radiused specimen is recommended.
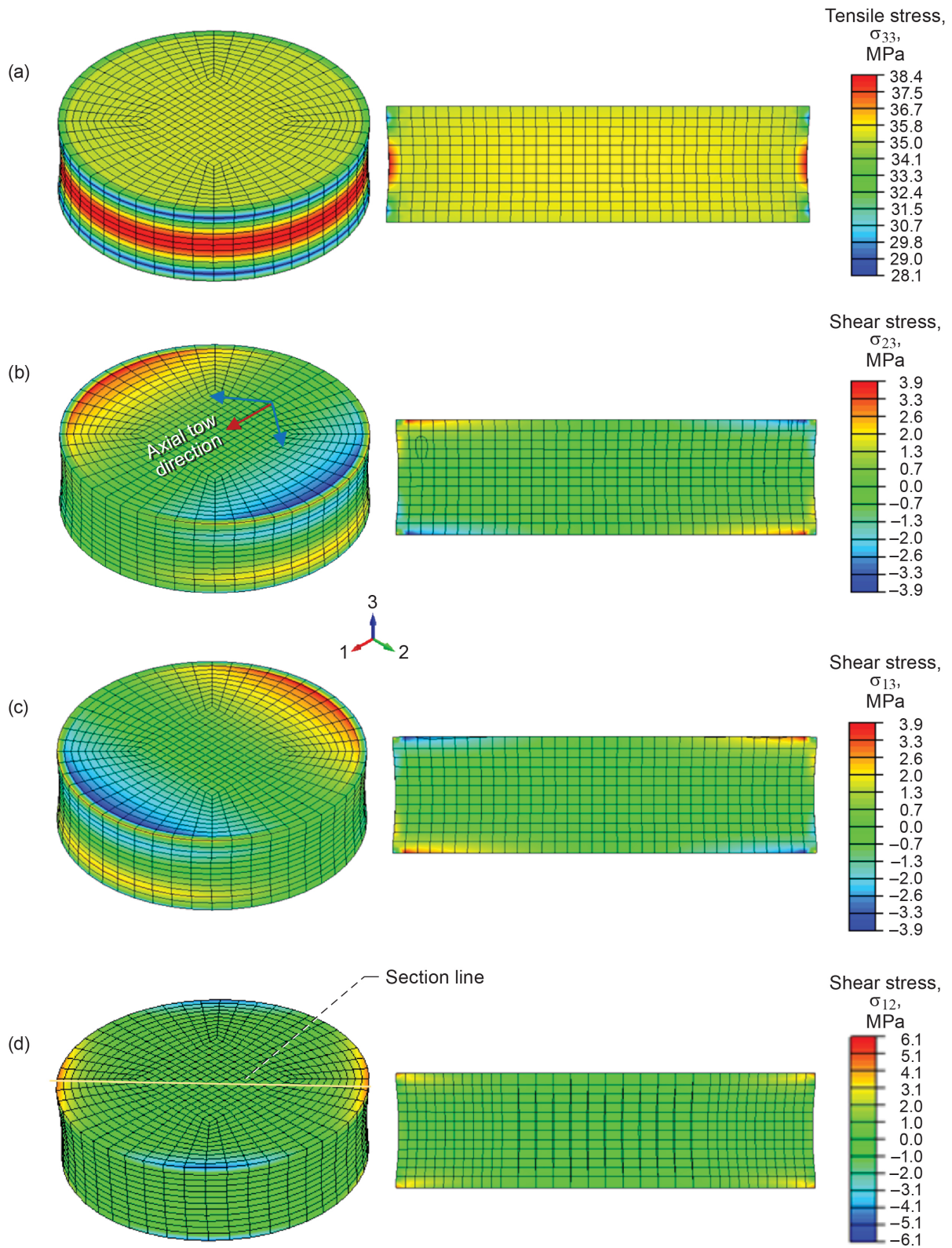
Figure 7.—Finite element analysis of radiused carbon/epoxy fiber composite. Tensile and shear distributions for global axial σ_{33} (Z) stress of 35 MPa. (a) σ_{33} stresses on perimeter and through the section. (b) σ_{23} shear stresses in first and second layers. (c) σ_{13} stresses. (d) σ_{12} stresses.
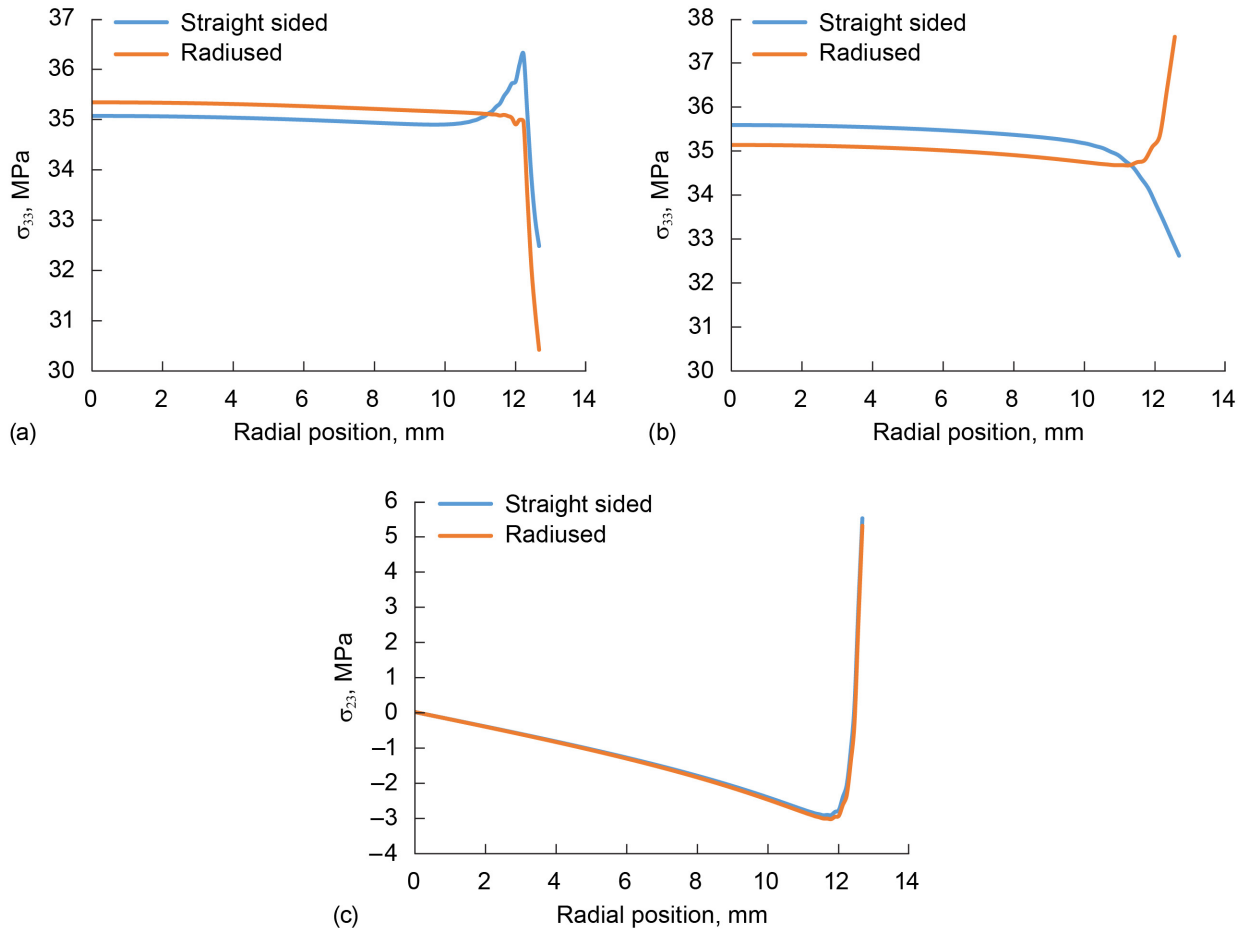
Figure 8.—Finite element analysis results of stress as function of radial position in top layer for straight-sided and radiused carbon/epoxy fiber composite test specimens. (a) Tensile stress σ_{33} at top layer. (b) Tensile stress σ_{33} at midplane. (c) Shear stress σ_{23} at top layer.

Failure Path

Fracture surfaces shown in Figure 9 exhibit smooth, undulating surfaces with varying degrees of fiber tear-out: for the T700S/PR520, fibers are pulled out in bands, whereas T700S/5208 exhibits wider, shallow damaged regions. The T700S/E863 exhibits behavior in between them. With the exception of a shallow layer of surface fibers, the tows remain intact, implying interlaminar failure. Comparison of matching halves reveals fiber and epoxy on one surface and an epoxy layer on the corresponding surface (Figure 10(a)). When scraped, the epoxy layer gives way to expose the fiber layer below (Figure 10(b)). Very few broken fibers are revealed at tow intersections, again implying interlaminar failure (Figure 10(c)) with little disturbance to axial tows.

Figure 11 shows a side view of the crack path as it undulates between stacked bias tows.
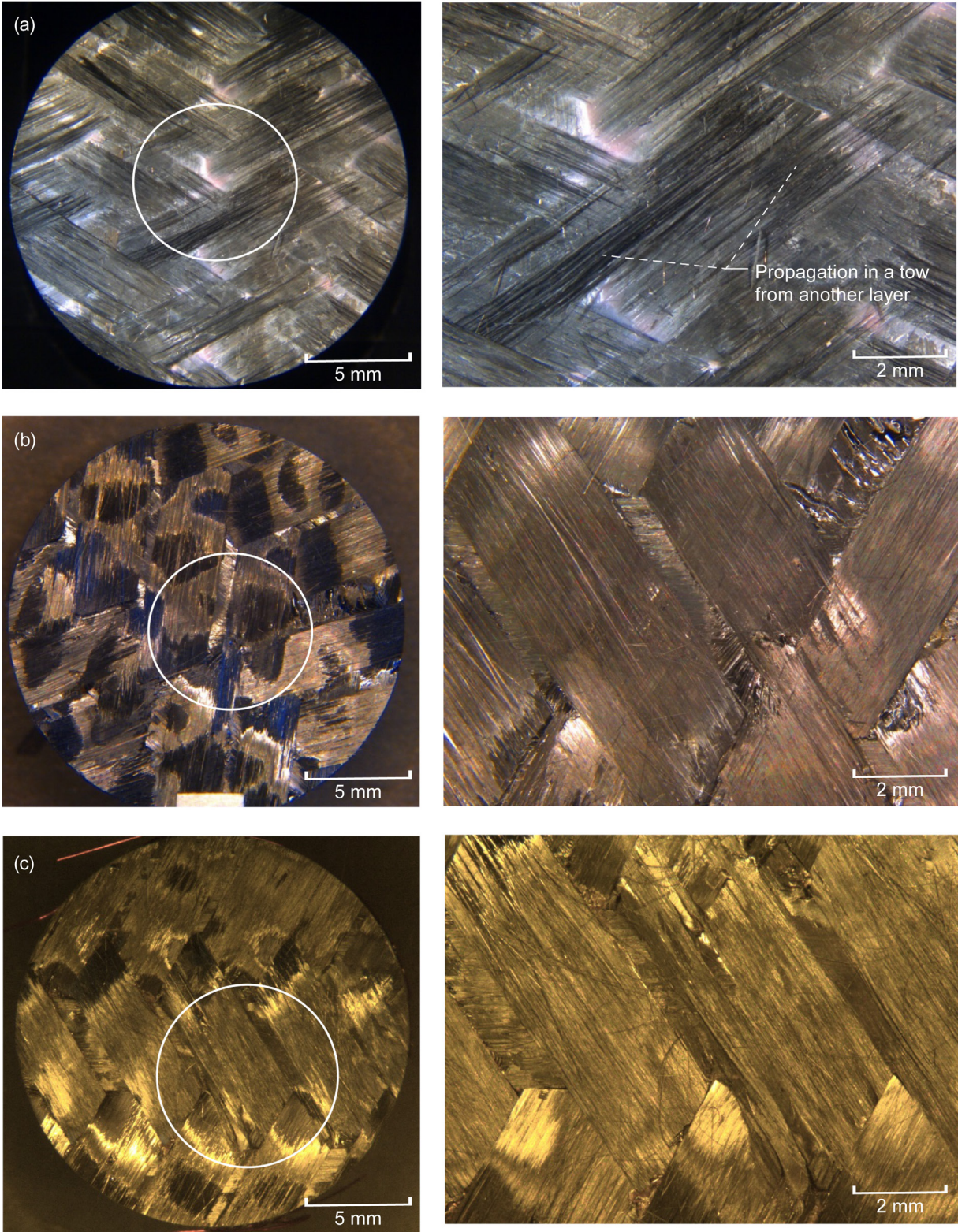
Figure 9.—Fracture surfaces of T700S carbon fiber composites with different epoxy resins. (a) PR520. (b) E862. (c) 5208.
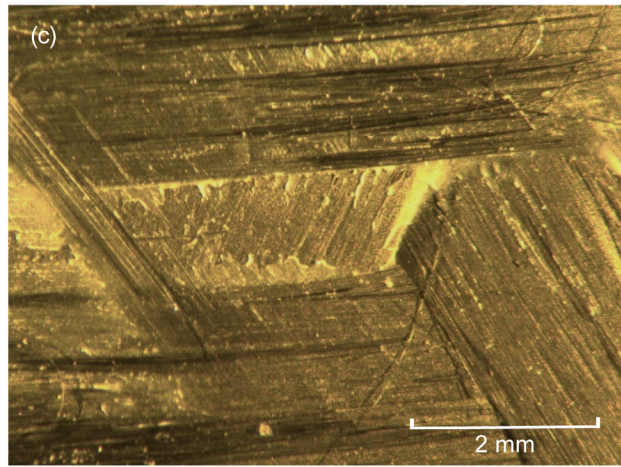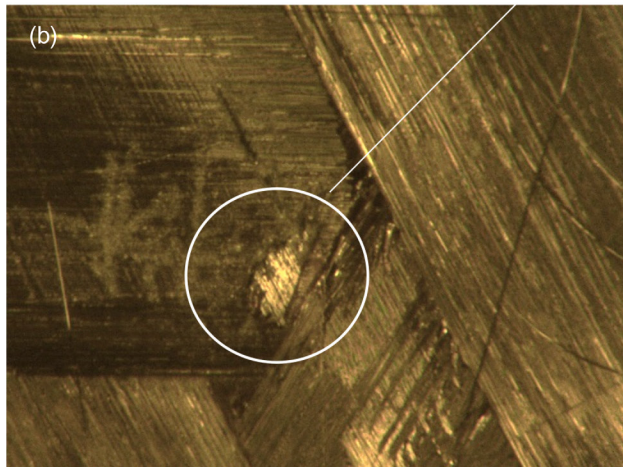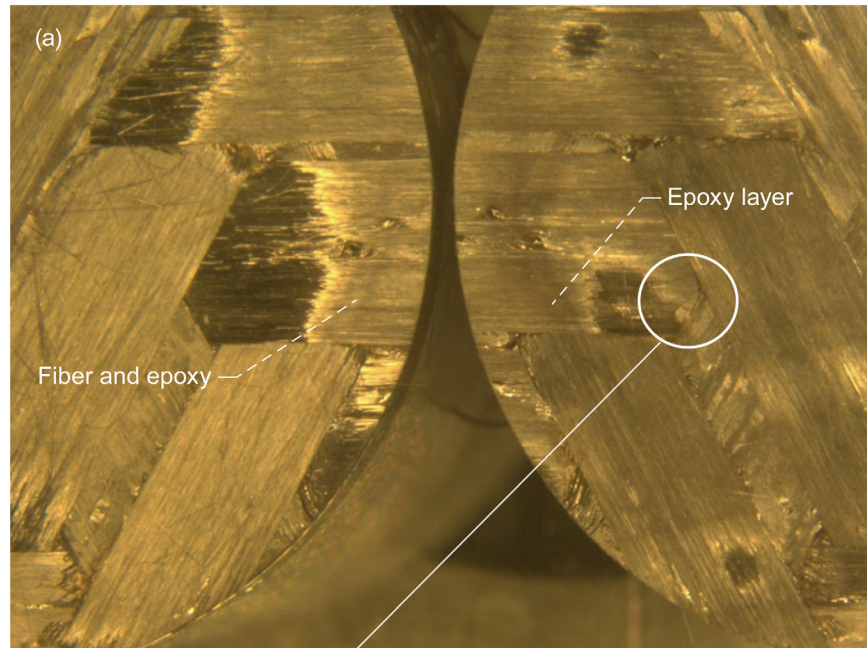
Figure 10.—Fractured T700S/5208 fiber composite. (a) Matching halves. (b) Scraping of film reveals fibers below. (c) Epoxy pocket in gaps between tows.
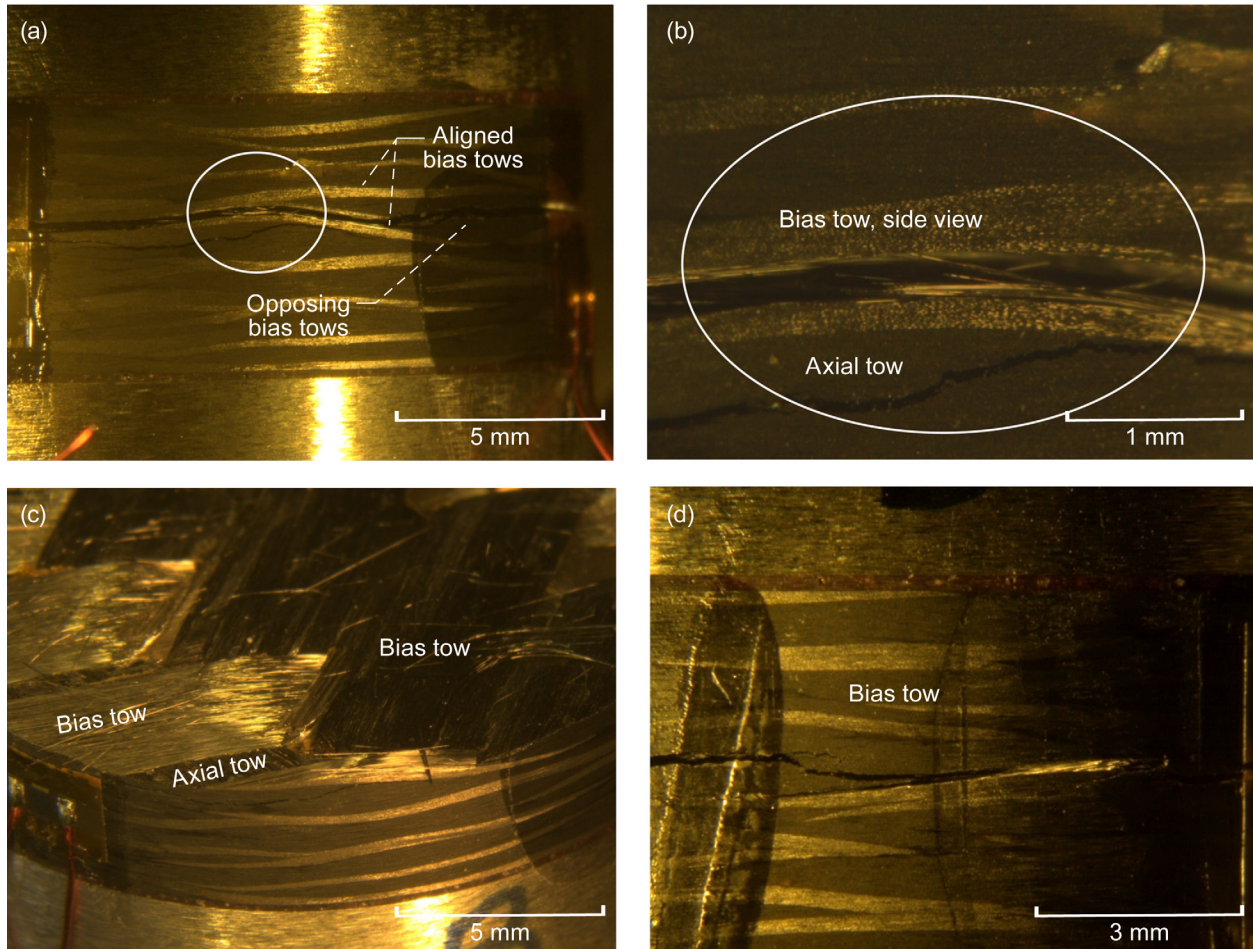
Figure 11.—Fractured T700S/5208 fiber composite. (a) Crack path between two aligned bias tows. (b) Magnification of circled portion in part (a). (c) Fracture surface showing tow orientation. (d) Delamination between opposing bias tows at different location.

Conclusions

Measurements of the through-thickness properties of triaxial braided composites by using thin specimens bonded to metallic tabs provided reasonable engineering estimates of the bulk properties. Some test specimen limitations were noted, however: For strong epoxies, significant combined shear and tensile stresses occur and induce failure between the first and second layers or at the bond line for straight-sided specimens; also, for straight-sided specimens the strains over much of the surface are ~6 percent lower than the interior strains, which are representative of the nominal state. Thermal strains may play a role, but further investigation of that is required.

Comparison of straight and radiused designs indicated that both geometries exhibit stress concentrations. The straight-sided design exhibited a small (4 percent) concentration near the adhesive bond, often producing bond-line failure. The radiused specimen exhibited a larger concentration (~10 percent) at centerline. The advantage of the radiused specimen is avoidance of bond-line failures, which tend to truncate strength distribution because the strongest specimens are eliminated. The radiused specimen is thus recommended for very strong systems.

Based on the finite element analysis and experimental measurements, the nominal elastic modulus and Poisson's ratio are $E_{33} = 10.7 \pm 0.8$ GPa and $\nu_{31} \approx \nu_{32} = 0.08 \pm 0.02$, respectively, for the three triaxial

braided composites employing T700S fiber and common epoxies. Reciprocity implies that $v_{13} \approx v_{23} \approx 0.4$. The through-thickness modulus, fracture strength, failure strain, and Poisson's ratio are 1/5, 1/30, 1/6, and 1/4 of the in-plane properties. Interlaminar failure occurred with varying amounts of bias fiber shredding and little damage to axial tows, resulting in a smooth, undulating fracture surface.

References

1. Littell, Justin D., et al.: Characterization of Damage in Triaxial Braid Composites Under Tensile Loading. NASA/TM—2009-215645, 2009. http://ntrs.nasa.gov
2. Salem, J.A., et al.: Burst Testing of Triaxial Braided Composite Tubes. NASA/TM—2014-216615, 2014. http://ntrs.nasa.gov
3. Roberts, Gary D., et al.: Characterization of Triaxial Braided Composite Material Properties for Impact Simulation. NASA/TM—2009-215660, 2009. http://ntrs.nasa.gov
4. Goldberg, Robert K., et al.: Analysis and Characterization of Damage Utilizing an Orthotropic Generalized Composite Material Model Suitable for Use in Impact Problems. NASA/TM—2016-218959, 2016. http://ntrs.nasa.gov
5. Littell, Justin D., et al.: Measurement of Epoxy Resin Tension, Compression, and Shear Stress-Strain Curves Over a Wide Range of Strain Rates Using Small Test Specimens. J. Aerospace Eng., vol. 21, no. 3, 2008, pp. 162−173.